MAX-PLANCK-INSTITUT
FÜR PLASMAPHYSIK

Modelling Shattered Pellet Injection in ASDEX Upgrade with DREAM

Peter Halldestam, Paul Heinrich, Gergely Papp,

Mathias Hoppe, Matthias Hölzl, István Pusztai, Oskar Vallhagen, Rainer Fischer,
Frank Jenko, the ASDEX Upgrade Team, and the EUROfusion Tokamak Exploitation Team

EUROfusion

This work has been carried out within the framework of the EUROfusion Consortium, funded by the European Union via the Euratom Research and Training Programme (Grant Agreement No 101052200 — EUROfusion). Views and opinions expressed are however those of the author(s) only and do not necessarily reflect those of the European Union or the European Commission. Neither the European Union nor the European Commission can be held responsible for them.

1) Background and motivation

Disruption simulation

- Disruption Runaway Electron Analysis Model (DREAM)

  [M. Hoppe *et al.*, CPC (2021)]

- SPI module

  [O. Vallhagen *et al.*, NF (2022)]

1) Background and motivation

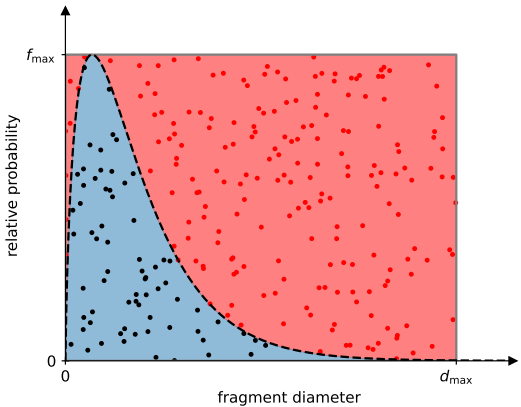

Disruption simulation

- Disruption Runaway Electron Analysis Model (DREAM)

  [M. Hoppe *et al.*, CPC (2021)]

- SPI module

  [O. Vallhagen *et al.*, NF (2022)]

Sampling fragments

- Parks' fragmentation model

  [P.B. Parks, GA Report (2016)]

  [T.E. Gebhart *et al.*, IEEE TPS (2019)]

- Fragment speed and direction

  [T. Peherstorfer, MSc thesis (2022)]

1) Background and motivation

Objectives

- Set up DREAM simulations modelling SPI in ASDEX Upgrade (AUG).
- Validate simulations with experiment.
- Assess impact of the statistical variation of the fragment distribution.

Outline

1. Background and motivation
2. Modelling of disruptions
3. Experimental comparison
   - Plasma current
   - Radiated energy fraction
4. Parameter scans
   - Ratio of injected Ne/D_2
   - Injection speed
5. Conclusion & Outlook

Outline

1. Background and motivation
2. Modelling of disruptions
3. Experimental comparison
   - Plasma current
   - Radiated energy fraction
4. Parameter scans
   - Ratio of injected Ne/D_2
   - Injection speed
5. Conclusion & Outlook

2.1) Modelling disruptions – MHD mixing

- **Plasma current** - via a mean-field equation [A.H. Boozer, NF (2018)]

$$\frac{\partial \psi_\mathrm{p}}{\partial t} = -V_\mathrm{loop} + \frac{\partial}{\partial \psi_\mathrm{t}} \left(\psi_\mathrm{t} \mu_0 \Lambda \frac{\partial}{\partial \psi_\mathrm{t}} \frac{j_\parallel}{B} \right) \tag{1}$$

2.1) Modelling disruptions – MHD mixing

- **Plasma current** - via a mean-field equation [A.H. Boozer, NF (2018)]

$$\frac{\partial \psi_\mathrm{p}}{\partial t} = -V_\mathrm{loop} + \frac{\partial}{\partial \psi_\mathrm{t}} \left(\psi_\mathrm{t} \mu_0 \Lambda \frac{\partial}{\partial \psi_\mathrm{t}} \frac{j_\parallel}{B} \right) \tag{1}$$

- **Energy balance**

$$\frac{3}{2} \frac{\partial n_\mathrm{e} T_\mathrm{e}}{\partial t} = \frac{1}{V'} \frac{\partial}{\partial r} \left[\frac{3 n_\mathrm{e}}{2} V' \chi_e \frac{\partial T_\mathrm{e}}{\partial r} \right] + \sigma_\parallel E_\parallel^2 - P_\mathrm{rad} + P_\mathrm{col} \tag{2}$$

2.1) Modelling disruptions – MHD mixing

- **Plasma current** - via a mean-field equation [A.H. Boozer, NF (2018)]

$$\frac{\partial \psi_\mathrm{p}}{\partial t} = -V_\mathrm{loop} + \frac{\partial}{\partial \psi_\mathrm{t}}\left(\psi_\mathrm{t}\mu_0\Lambda\frac{\partial}{\partial \psi_\mathrm{t}}\frac{j_\parallel}{B}\right) \tag{1}$$

- **Energy balance**

$$\frac{3}{2}\frac{\partial n_\mathrm{e} T_\mathrm{e}}{\partial t} = \frac{1}{V'}\frac{\partial}{\partial r}\left[\frac{3n_\mathrm{e}}{2}V'\chi_e\frac{\partial T_\mathrm{e}}{\partial r}\right] + \sigma_\parallel E_\parallel^2 - P_\mathrm{rad} + P_\mathrm{col} \tag{2}$$

- **Ion charge state evolution**

$$\frac{\partial n_i^{(j)}}{\partial t} = \frac{1}{V'}\frac{\partial}{\partial r}V'\left(A_i n_i^{(j)} + D_i\frac{\partial n_i^{(j)}}{\partial r}\right) + \left.\frac{\partial n_i^{(j)}}{\partial t}\right|_\mathrm{ionis} + \left.\frac{\partial n_i^{(j)}}{\partial t}\right|_\mathrm{SPI} \tag{3}$$

2.1) Modelling disruptions – MHD mixing

- **Plasma current** - via a mean-field equation [A.H. Boozer, NF (2018)]

$$\frac{\partial \psi_\mathrm{p}}{\partial t} = -V_\mathrm{loop} + \frac{\partial}{\partial \psi_\mathrm{t}} \left(\psi_\mathrm{t} \mu_0 \Lambda \frac{\partial}{\partial \psi_\mathrm{t}} \frac{j_\parallel}{B} \right) \tag{1}$$

- **Energy balance**

$$\frac{3}{2} \frac{\partial n_\mathrm{e} T_\mathrm{e}}{\partial t} = \frac{1}{V'} \frac{\partial}{\partial r} \left[\frac{3 n_\mathrm{e}}{2} V' \chi_e \frac{\partial T_\mathrm{e}}{\partial r} \right] + \sigma_\parallel E_\parallel^2 - P_\mathrm{rad} + P_\mathrm{col} \tag{2}$$

- **Ion charge state evolution**

$$\frac{\partial n_i^{(j)}}{\partial t} = \frac{1}{V'} \frac{\partial}{\partial r} V' \left(A_i n_i^{(j)} + D_i \frac{\partial n_i^{(j)}}{\partial r} \right) + \left. \frac{\partial n_i^{(j)}}{\partial t} \right|_\mathrm{ionis} + \left. \frac{\partial n_i^{(j)}}{\partial t} \right|_\mathrm{SPI} \tag{3}$$

2.1) Modelling disruptions – MHD mixing

- **Enhanced transport** – Coefficients: $\mathcal{Y} \in \{\chi_e,\ D_i,\ A_i, \Lambda\}$.

$$\frac{\mathcal{Y}(t)}{\mathcal{Y}_{\max}} = \exp\left(-\frac{t - t_{\text{relax}}}{\tau_{\text{down}}}\right)\Theta(t - t_{\text{relax}}). \tag{4}$$

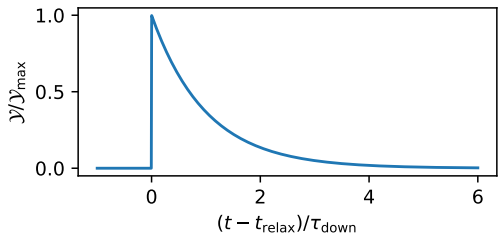

2.1) Modelling disruptions – MHD mixing

- **Enhanced transport** – Coefficients: $\mathcal{Y} \in \{\chi_e,\ D_i,\ A_i, \Lambda\}$.

$$\frac{\mathcal{Y}(t)}{\mathcal{Y}_{\max}} = \exp\left(-\frac{t - t_{\text{relax}}}{\tau_{\text{down}}}\right)\Theta(t - t_{\text{relax}}). \tag{4}$$

- **Relaxation trigger criterion** – We set t_{relax} to the time t at which the electron temperature $T_e < 10\,\text{eV}$ for any radial point within the $q = 2$ surface.

2.1) Modelling disruptions – MHD mixing

- **Enhanced transport** – Coefficients: $\mathcal{Y} \in \{\chi_e,\ D_i,\ A_i, \Lambda\}$.

$$\frac{\mathcal{Y}(t)}{\mathcal{Y}_{\max}} = \exp\left(-\frac{t - t_{\text{relax}}}{\tau_{\text{down}}}\right)\Theta(t - t_{\text{relax}}). \tag{4}$$

- **Relaxation trigger criterion** – We set t_{relax} to the time t at which the electron temperature $T_e < 10\,\text{eV}$ for any radial point within the $q = 2$ surface.
- **Free parameters**
  - $\tau_{\text{down}} = 1\,\text{ms}$.
  - $\chi_{e,\max},\ D_{i,\max} = 10^2\,\text{m}^2/\text{s},\ A_{i,\max} = -10^2\,\text{m/s}$ [O. Linder *et al.* NF 2020]
  - $\Lambda_{\max} = 10^{-5}\,\text{Wb}^2\text{m/s}$ *matching* with experimentally observed I_{p} spikes.

2.2) Modelling disruptions – Input data

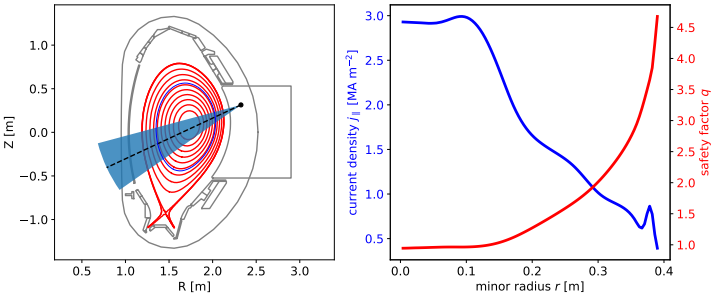

- Reference AUG shot #40665 @$t = 2.305\,\mathrm{s}$.
- Ohmic current as total current, not modelling NBCD & bootstrap current.

2.2) Modelling disruptions – Input data

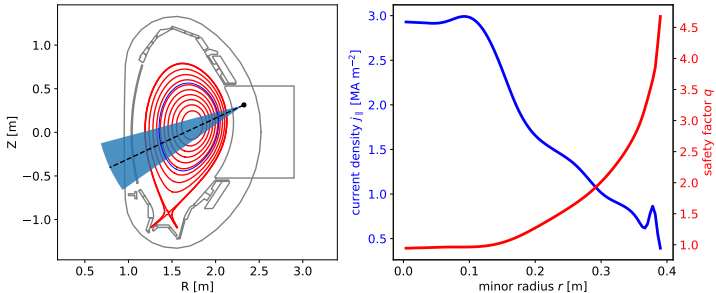

- Reference AUG shot #40665 @$t = 2.305\,\mathrm{s}$.
- Ohmic current as total current, not modelling NBCD & bootstrap current.
- $8 \times 9.5\,\mathrm{mm}$ pellets, 25° angle, $v_\mathrm{inj} = 230\,\mathrm{m/s}$, $f_\mathrm{Ne} = 10\,\%$ Ne/D_2-pellet, fragment plume $N_\mathrm{frag} \sim 100$, $\langle v_\mathrm{frag} \rangle = 220\,\mathrm{m/s}$, $\Delta v_\mathrm{frag} / \langle v_\mathrm{frag} \rangle = 20\,\%$, $\theta_\mathrm{plume} = 20°$.

2.2) Modelling disruptions – Input data

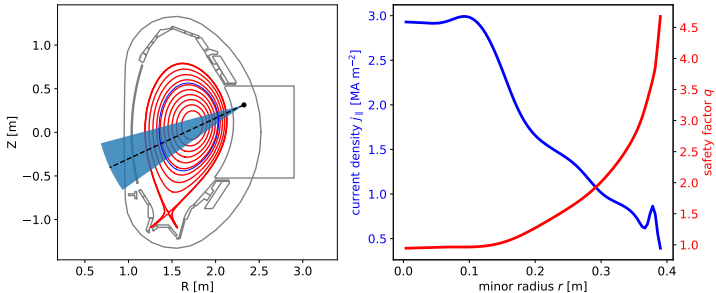

- Reference AUG shot #40665 @$t = 2.305\,\mathrm{s}$.
- Ohmic current as total current, not modelling NBCD & bootstrap current.
- $8 \times 9.5\,\mathrm{mm}$ pellets, 25° angle, $v_\mathrm{inj} = 230\,\mathrm{m/s}$, $f_\mathrm{Ne} = 10\,\%$ Ne/D_2-pellet, fragment plume $N_\mathrm{frag} \sim 100$, $\langle v_\mathrm{frag} \rangle = 220\,\mathrm{m/s}$, $\Delta v_\mathrm{frag} / \langle v_\mathrm{frag} \rangle = 20\,\%$, $\theta_\mathrm{plume} = 20°$.

2.2) Modelling disruptions – Input data

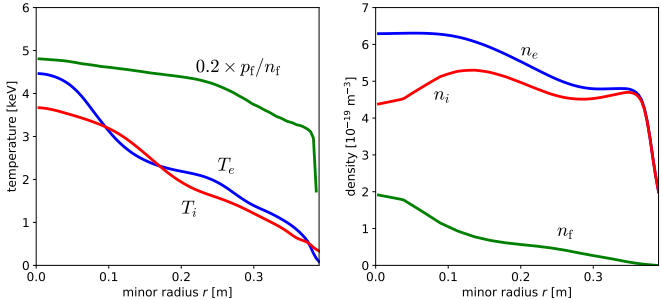

- Input equilibrium and profiles from IDA.

  [R. Fischer *et al.* Plasma Phys. Control. Fusion (2010)]

- Non-negligible population of non-Maxwellian fast ions due to NBI.

2.2) Modelling disruptions – Input data

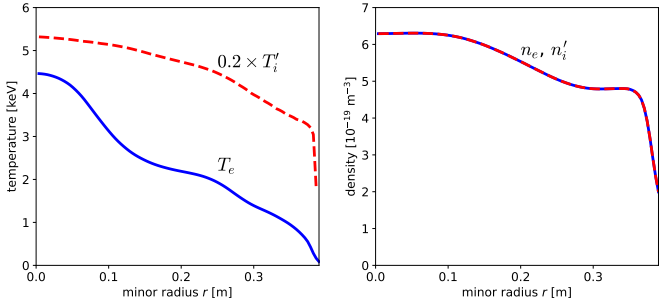

- Input equilibrium and profiles from IDA.

  [R. Fischer *et al.* Plasma Phys. Control. Fusion (2010)]

- Non-negligible population of non-Maxwellian fast ions due to NBI.
- We assume an instantaneous thermalisation of all fast particles at $t = 0$.

2.3) Modelling disruptions – Example simulation

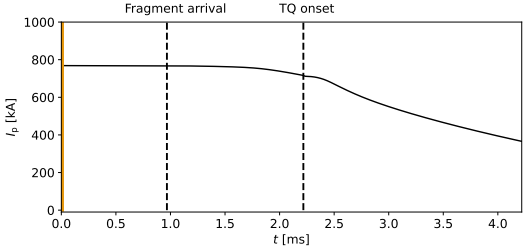

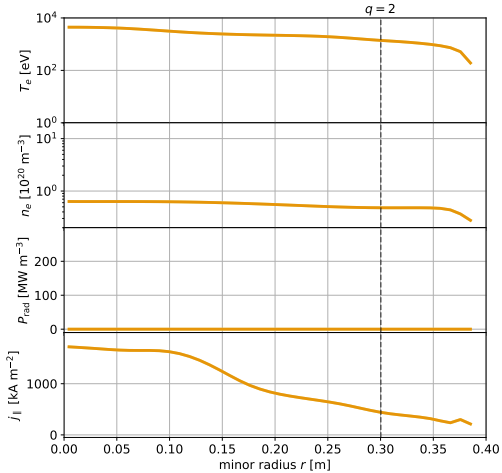

2.3) Modelling disruptions – Example simulation

- Fragment arrival, dilution cooling.

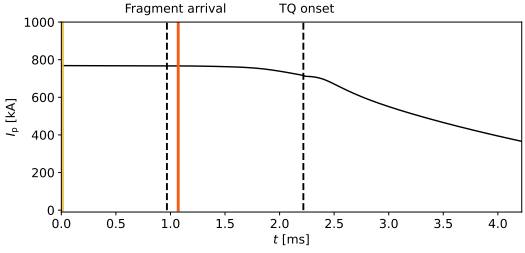

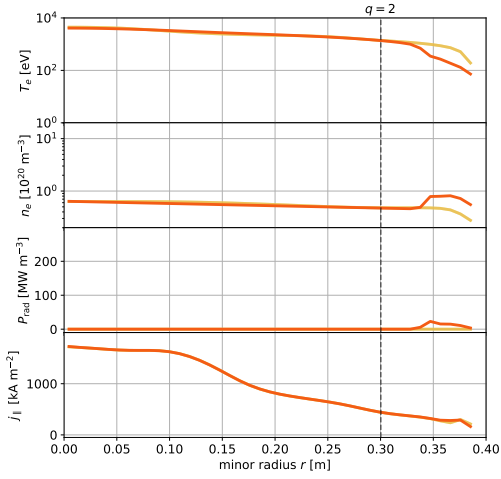

2.3) Modelling disruptions – Example simulation

- Fragment arrival, dilution cooling.
- Radiative cooling, cold front forms.

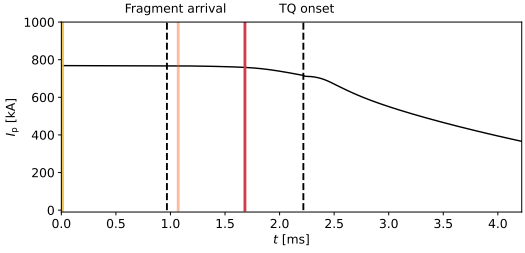

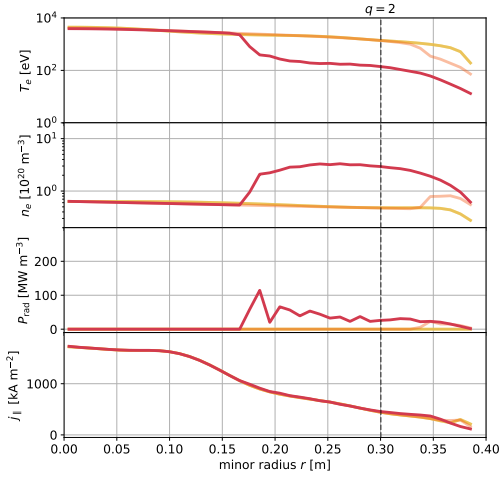

2.3) Modelling disruptions – Example simulation

- Fragment arrival, dilution cooling.
- Radiative cooling, cold front forms.

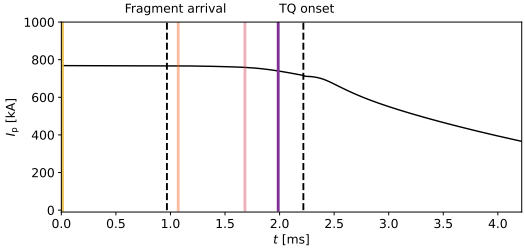

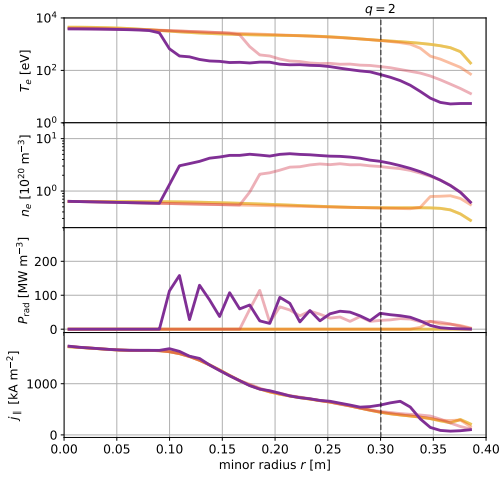

2.3) Modelling disruptions – Example simulation

- Fragment arrival, dilution cooling.
- Radiative cooling, cold front forms.
- Cold front reaches resonant surface.

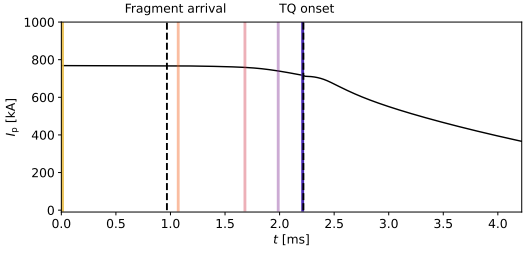

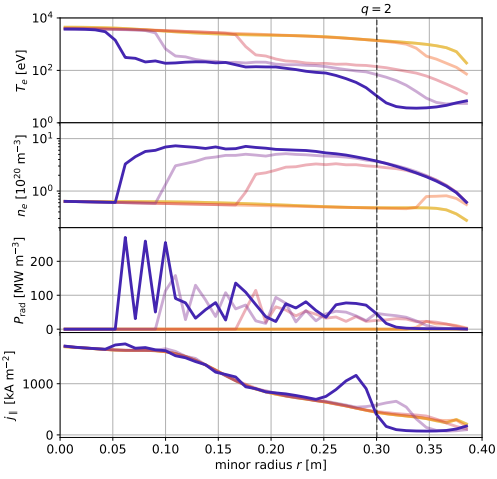

2.3) Modelling disruptions – Example simulation

- Fragment arrival, dilution cooling.
- Radiative cooling, cold front forms.
- Cold front reaches resonant surface.
- Relaxation of profiles, current spike.

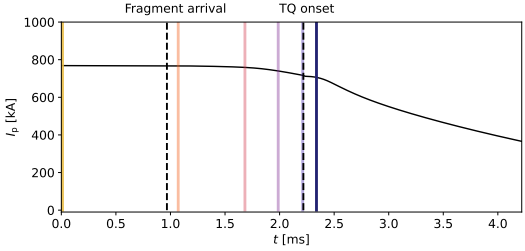

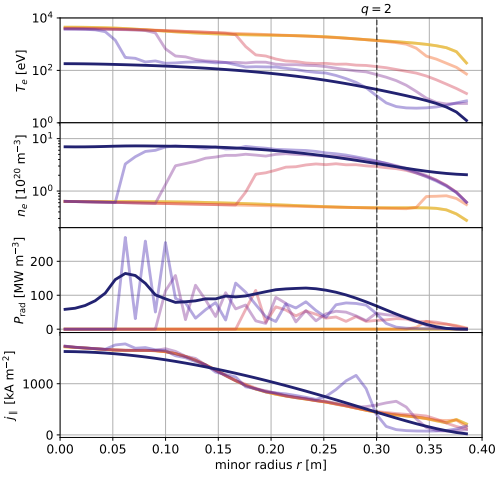

2.3) Modelling disruptions – Example simulation

- Fragment arrival, dilution cooling.
- Radiative cooling, cold front forms.
- Cold front reaches resonant surface.
- Relaxation of profiles, current spike.
- Current quench.

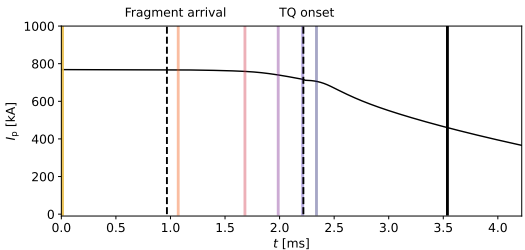

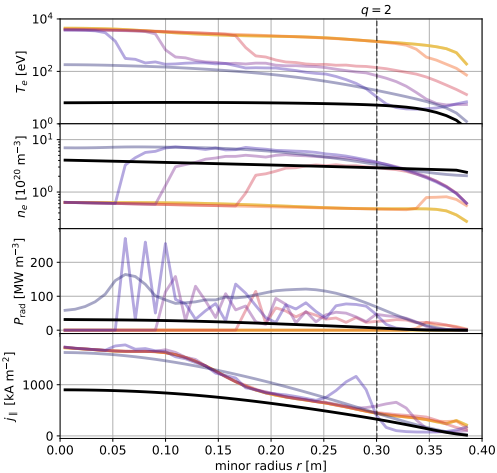

Outline

1. Background and motivation
2. Modelling of disruptions
3. Experimental comparison
   - Plasma current
   - Radiated energy fraction
4. Parameter scans
   - Ratio of injected Ne/D_2
   - Injection speed
5. Conclusion & Outlook

3.1) Experimental comparison – Plasma current

- 6 AUG shots, varying f_{Ne}.

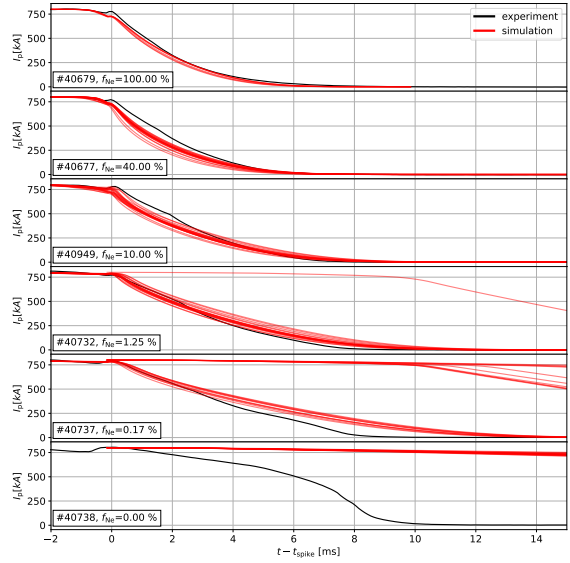

3.1) Experimental comparison – Plasma current

- 6 AUG shots, varying f_{Ne}.
- Good agremeent with experiment.

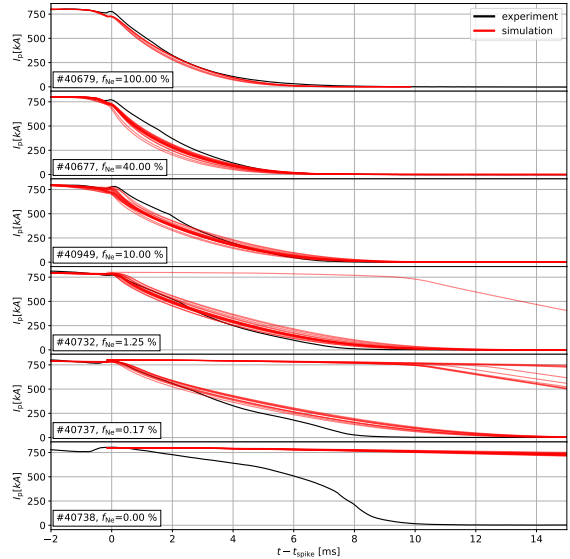

3.1) Experimental comparison – Plasma current

- 6 AUG shots, varying f_{Ne}.
- Good agremeent with experiment.
- TQ not always triggered for low f_{Ne} SPI.

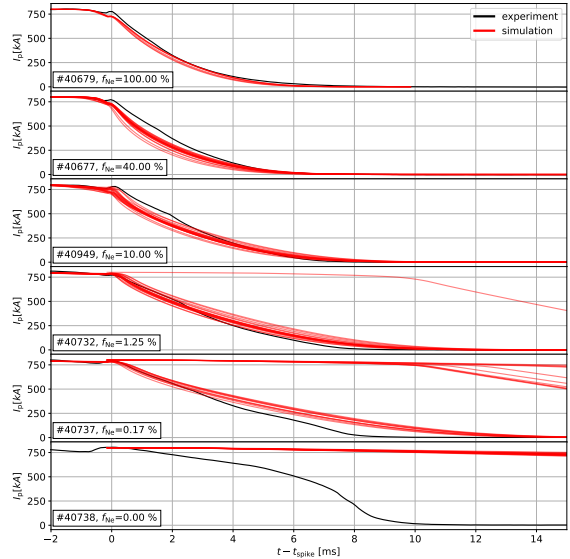

3.1) Experimental comparison – Plasma current

- 6 AUG shots, varying f_{Ne}.
- Good agremeent with experiment.
- TQ not always triggered for low f_{Ne} SPI.
- Disruption in #40738 is not triggered by the control system.

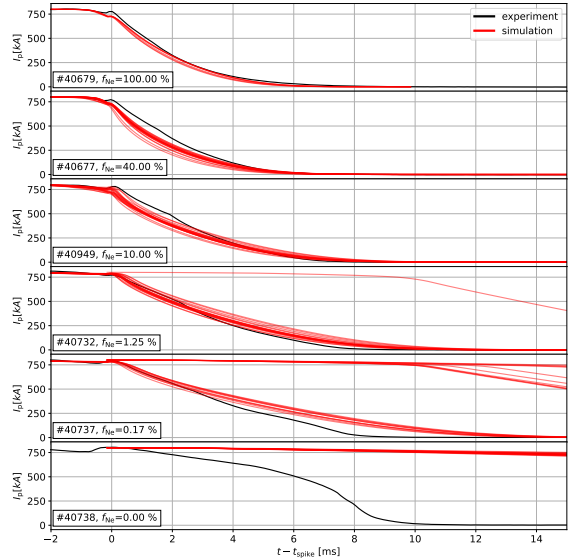

3.1) Experimental comparison – Plasma current

- 6 AUG shots, varying f_{Ne}.
- Good agremeent with experiment.
- TQ not always triggered for low f_{Ne} SPI.
- Disruption in #40738 is not triggered by the control system.
- Impurities are not included in the simulations.

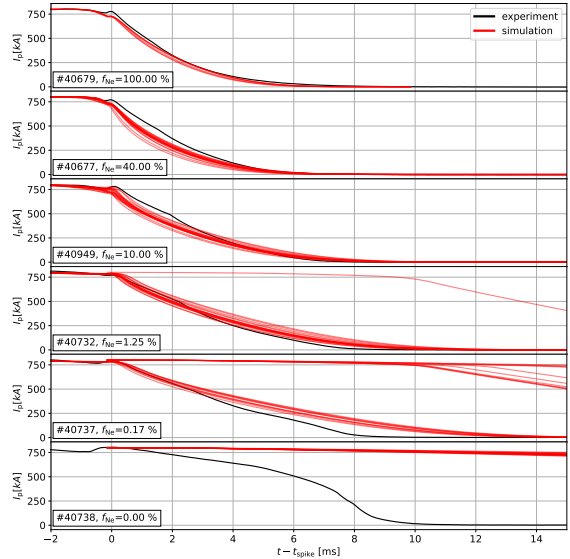

3.2) Experimental comparison – Radiated energy fraction

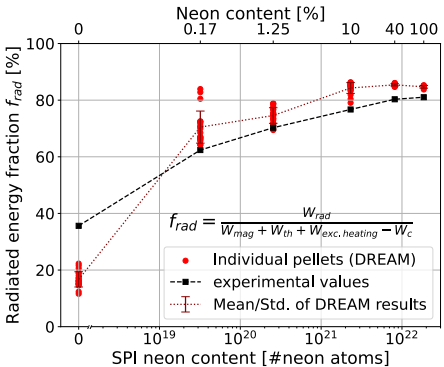

- Agrees well with experimental estimates.

  [P. Heinrich *et al.*, NF paper in preparation]

3.2) Experimental comparison – Radiated energy fraction

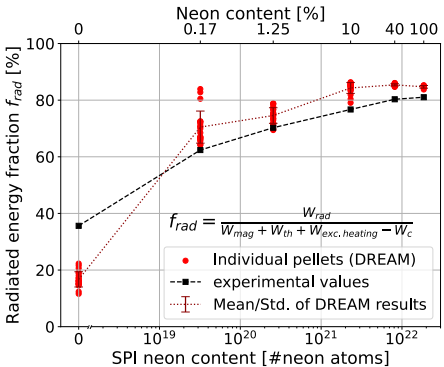

- Agrees well with experimental estimates.
  [P. Heinrich *et al.*, NF paper in preparation]
- Saturates at $f_{\mathrm{Ne}} \sim 10\,\%$.

3.2) Experimental comparison – Radiated energy fraction

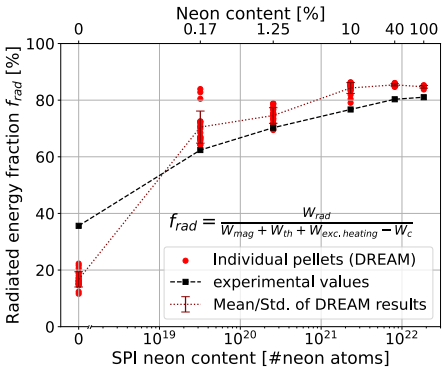

- Agrees well with experimental estimates.
  [P. Heinrich *et al.*, NF paper in preparation]
- Saturates at $f_{\mathrm{Ne}} \sim 10\,\%$.
- Strongest impact of statistics at $0.17\,\%$.

3.2) Experimental comparison – Radiated energy fraction

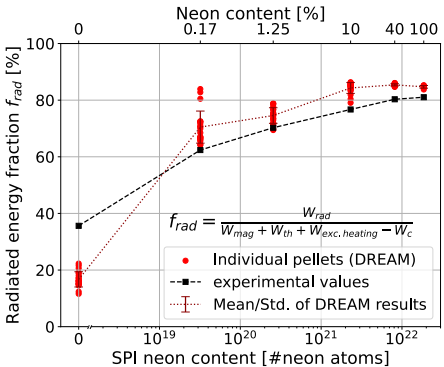

- Agrees well with experimental estimates.
  [P. Heinrich *et al.*, NF paper in preparation]
- Saturates at $f_{\mathrm{Ne}} \sim 10\,\%$.
- Strongest impact of statistics at $0.17\,\%$.
- Underestimates for pure D_2 pellets.

Outline

1. Background and motivation
2. Modelling of disruptions
3. Experimental comparison
   - Plasma current
   - Radiated energy fraction
4. Parameter scans
   - Ratio of injected Ne/D_2
   - Injection speed
5. Conclusion & Outlook

4.1) Neon fraction scan – Plasma current and thermal energy

SPI parameters

25° shatter angle,
$8 \times 9.5\,\mathrm{mm}$ pellets,
scan in f_{Ne},
$v_{\mathrm{inj}} = 230\,\mathrm{m/s}$,
$\langle v_{\mathrm{frag}} \rangle = 220\,\mathrm{m/s}$,
$\Delta v_{\mathrm{frag}} / \langle v_{\mathrm{frag}} \rangle = 20\,\%$,
$\theta_{\mathrm{plume}} = 20°$.

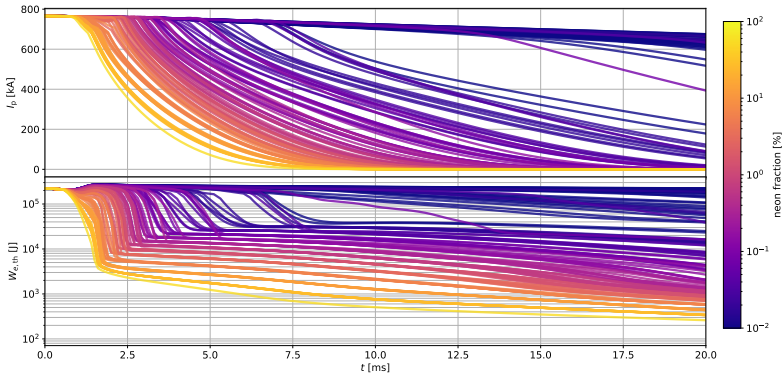

4.1) Neon fraction scan – Radiated energy fraction

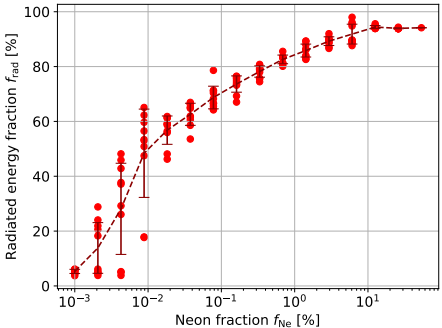

- Preliminary results.
- Calculating f_{rad} for non-disruptive cases can be somewhat tricky…
- Strongest impact of statistics for $f_{\mathrm{Ne}} \lesssim 0.01\,\%$.

4.2) Injection speed scan – Plasma current and thermal energy

SPI parameters

25° shatter angle,
$8 \times 9.5\,\mathrm{mm}$ pellets,
$f_{\mathrm{Ne}} = 10\,\%$,
scan in v_{inj},
$\langle v_{\mathrm{frag}} \rangle \propto v_{\mathrm{inj}}$,
$\Delta v_{\mathrm{frag}} / \langle v_{\mathrm{frag}} \rangle = 20\,\%$,
$\theta_{\mathrm{plume}} = 20^\circ$.

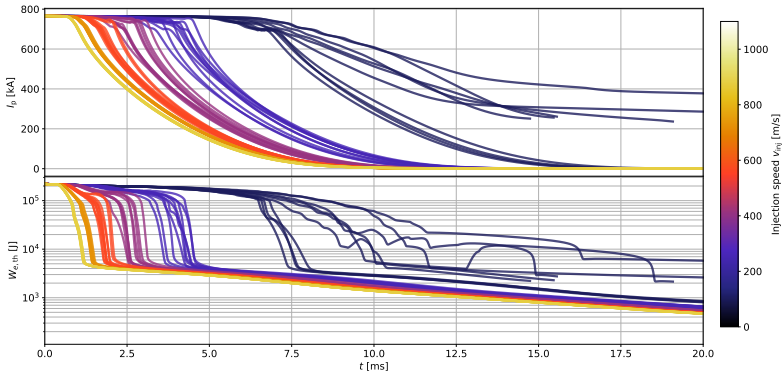

4.2) Injection speed scan – Radiated energy fraction

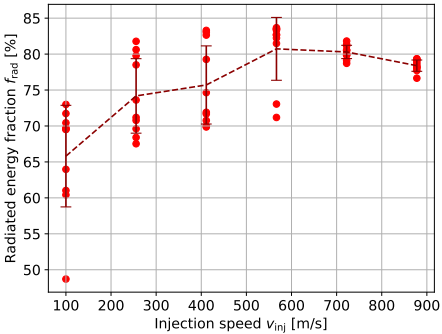

- Both N_{frag} and v_{frag} depend on v_{inj}.

4.2) Injection speed scan – Radiated energy fraction

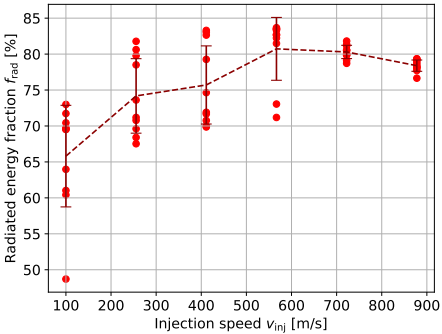

- Both N_{frag} and v_{frag} depend on v_{inj}.
- Slowest generate $N_{\text{frag}} \sim 5$, while fastest $N_{\text{frag}} \sim 2000$.

4.2) Injection speed scan – Radiated energy fraction

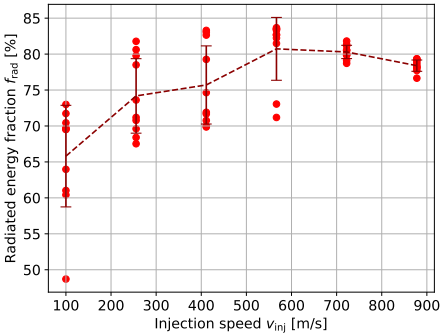

- Both N_{frag} and v_{frag} depend on v_{inj}.
- Slowest generate $N_{\mathrm{frag}} \sim 5$, while fastest $N_{\mathrm{frag}} \sim 2000$.
- Optimal range $600 - 700\,\mathrm{m/s}$?
- Gas generation not modelled.

4.2) Injection speed scan – Radiated energy fraction

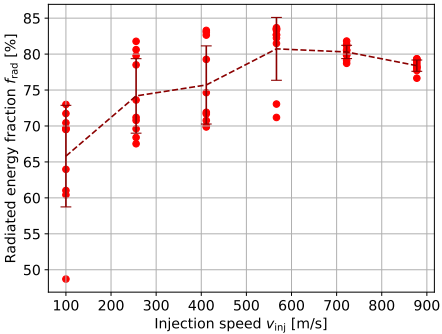

- Both N_{frag} and v_{frag} depend on v_{inj}.
- Slowest generate $N_{\text{frag}} \sim 5$, while fastest $N_{\text{frag}} \sim 2000$.
- Optimal range $600 - 700\,\text{m/s}$?
- Gas generation not modelled.
- In reality, v_{inj} limited by the speed of sound of the propellant gas.

Conclusion

- Modelling AUG SPI disruption discharges with DREAMsimulations.
- Good agreement with I_p compared to experiment, except for the lowest neon fractions.
- Good agreement with experimentally measured f_rad and its scaling with f_Ne.
- Small impact of the statistical variation in the shard size distribution on f_rad, except for cases with trace amounts of neon.
- Negligible amount of RE current observed, consistently with experiment.

Outlook

- ❏ Investigate effect of impurities.
  [J. Walkowiak *et al.*, NF (2024)]
- ❏ Scan injection parameters, e.g. injection speed, plume spread...
- ❏ Use experimental fragments distributions.
  [J. Illerhaus *et al.*, J. Fusion Energy (2024)]
- ❏ Include plasmoid drift model.
  [O. Vallhagen *et al.*, JPP (2023)]

Verification/Validation:

- ❏ JOREK (W. Tang), INDEX (A.H. Patel)
- ❏ Compare P_{rad} with bolometry data.
- ❏ Compare n_{e} with line-integrated density measurements.

Back-up slides

Combining thermal and fast ions

- Thermalisation of fast ions:

$$n_i' T_i' = n_i T_i + p_\mathrm{f} \tag{5}$$

- Assume pure D_2 plasma and quasi-neutrality:

$$n_i' = n_i + n_\mathrm{f} = n_\mathrm{e} \tag{6}$$

Together, these assumptions yields the following rescaling in ion temperature:

$$\implies T_i' = \left(1 + \frac{n_\mathrm{f}}{n_\mathrm{e}}\right) T_i + \frac{p_\mathrm{f}}{n_\mathrm{e}} \tag{7}$$

Sampling shard velocities

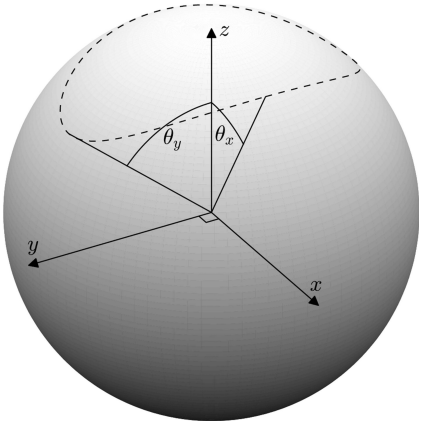

source: Hall 2017

For each shard, a velocity $\boldsymbol{v}_{\text{frag}}$ is assigned.

- Speed $v = |\boldsymbol{v}_{\text{frag}}|$ follow a Gaussian distribution.
- Direction $\hat{v}_{\text{frag}} = \boldsymbol{v}_{\text{frag}}/v_{\text{frag}}$ distributed on the unit sphere within an elliptical cone.

  [Hall, CPC (2017)].
- Spatial spread from lab data.

  [Peherstorfer, MSc thesis (2022)]

DREAM: – SPI module

- **Neutral Gas Shielding model** [Parks & Turnbull, PoF (1978)]]

$$\dot{r}_{\mathrm{s},k} \propto -q_{\mathrm{e}}^{1/3} T_{\mathrm{e}}^{7/6} r_{\mathrm{s},k}^{4/3} \tag{8}$$

- **Deposition of ablated material into the plasma** [Vallhagen *et al.*, NF (2022)]

$$\left.\frac{\partial n_i^{(j)}}{\partial t}\right|_{\mathrm{SPI}} = -\delta_{0j} \sum_{k=1}^{N_{\mathrm{s}}} \frac{4\pi r_{\mathrm{s},k}^2 \dot{r}_{\mathrm{s},k} \rho_{\mathrm{mass}} N_{\mathrm{A}}}{\mathcal{M}} H(r, \rho_{\mathrm{s},k}) \tag{9}$$

DREAM – Runaway electrons

- **Continuity equation** $\implies n_{\mathrm{re}}$

$$\frac{\partial n_{\mathrm{re}}}{\partial t} = \frac{1}{V'}\frac{\partial}{\partial r}\left[V' D_{\mathrm{re}} \frac{\partial n_{\mathrm{re}}}{\partial r}\right] + \gamma_{\mathrm{Dreicer}} + \gamma_{\mathrm{hot-tail}} + \Gamma_{\mathrm{ava}} n_{\mathrm{re}} \tag{10}$$

- Dreicer mechanism neural network

  [Hesslow *et al.*, JPP (2019)]

- Hot-tail mechanism

  [Svenningsson, MSc thesis (2020)]

- Avalanche generation

  [Hesslow *et al.*, NF (2019)]

DREAM – Thermal particles

- **Energy balance** $\implies n_\mathrm{e}\, T_\mathrm{e}$

$$\frac{3}{2}\frac{\partial n_\mathrm{e} T_\mathrm{e}}{\partial t} = \frac{1}{V'}\frac{\partial}{\partial r}\left[\frac{3n_\mathrm{e}}{2} V' \chi \frac{\partial T_\mathrm{e}}{\partial r}\right] + P_\Omega - P_\mathrm{rad} + P_\mathrm{re} + \sum_i Q_{ei}. \tag{11}$$

- **Quasi-neutrality** $\implies n_\mathrm{e}$

$$\sum_i \sum_{j=1}^{Z_i} Z_{0j}\, n_i^{(j)} - n_\mathrm{e} - n_\mathrm{re} = 0. \tag{12}$$

- **Collisional heat exchange** $\implies W_i$

$$\frac{\partial W_i}{\partial t} = Q_{ie} + \sum_{i' \neq i} Q_{ii'}. \tag{13}$$

DREAM – Ion charge states

- **Continuity equation** $\implies n_i^{(j)}$

$$\frac{\partial n_i^{(j)}}{\partial t} = \frac{1}{V'}\frac{\partial}{\partial r} V' \left(A_i n_i^{(j)} + D_i \frac{\partial n_i^{(j)}}{\partial r} \right) + \left.\frac{\partial n_i^{(j)}}{\partial t}\right|_{\text{ionis}} + \left.\frac{\partial n_i^{(j)}}{\partial t}\right|_{\text{SPI}}. \tag{14}$$

- **Ionisation & recombination**

$$\left.\frac{\partial n_i^{(j)}}{\partial t}\right|_{\text{ionis}} = n_{\text{e}} \left[\mathcal{I}_i^{(j-1)} n_i^{(j-1)} + \left(\mathcal{I}_i^{(j)} + \mathcal{R}_i^{(j)} \right) n_i^{(j)} + \mathcal{R}_i^{(j+1)} n_i^{(j+1)} \right] \tag{15}$$

- **Deposition of ablated material**

$$\left.\frac{\partial n_i^{(j)}}{\partial t}\right|_{\text{SPI}} = -\delta_{0j} \sum_{k=1}^{N_{\text{s}}} \frac{4\pi r_{\text{s},k}^2 \dot{r}_{\text{s},k} \rho_{\text{mass}} N_{\text{A}}}{\mathcal{M}} H(r, \rho_{\text{s},k}) \tag{16}$$